Pakistan Journal of Applied Sciences 1 (4): 472-476, 2001

Compressible Flow Around A Circular Cylinder

Ebrahim Shirani
Mechanical Engineering Department, Isfahan University of Technology
Isfahan, Iran

Abstract: Viscous compressible flow around a circular cylinder is numerically simulated. The inflow Mach numbers and Reynolds numbers of the flow are from 0.1 to 0.9 and 10^3 to 8.4 X 10^6 respectively. Two-dimensional time averaged Navier-Stokes equations were numerically solved. The Beam-Warming type numerical method was employed on two different C- and O-type meshes. The effects of Mach and Reynolds numbers on the flow parameters such as drag and lift coefficients, and the formation and growth of the vortices were investigated. It is found that for Mach numbers above about 0.6, the flow parameters become independent of Reynolds number and at about this Mach number, due to the formation of shock waves, the flow characteristics change rapidly with Mach number. But as Mach number becomes greater than 0.8 (0.8<M<1.0), the flow becomes independent of Mach number. In some cases, where experimental results were available, the results were compared and good agreement was obtained.

Keywords: Compressible Flow, Cylinder, Drag Coefficient, Lift Coefficient

Introduction

Due to its vast engineering applications and also its potential to investigate some important aspects of fluid dynamics in such a simple geometry, the flow around circular cylinders have been focus of much attention in the past few decades. Cantwell and Coles, (1983) have presented a large list of papers in this regard.

The behavior of the flow around circular cylinder with Reynolds numbers between 10^3 and 10^6 has special features of interest. The unsteady nature of the flow behind the cylinder, the generation and growth of the vortices, the location of separation point and the size of the wake behind the cylinder are among the subjects to investigate.

Much of the attention has been put into the incompressible case. Despite the large number of independent numerical and experimental studies in the incompressible case, there are some uncertainties about the drag and shedding frequency for the flow over a circular cylinder. For compressible case when the inflow Mach number becomes larger than about 0.5, the flow become locally supersonic and shock waves occur. The shock waves cause large pressure gradient near the surface and change the location of the separation points and the structures of the flow. Therefore, the drag coefficient and pressure distributions around the cylinder change. The aim of this paper is to investigate the effects of Mach and Reynolds numbers on the flow characteristics around a circular cylinder. The effects of compressibility on the subsonic flow around the cylinder were considered by some investigators (such as Ferri (1942), Schulle-Werning *et al.* (1990), Song *et al.* (1990), and Farel and Blessmann (1983). But there is not rather complete set of data over a large range of Mach numbers (0.1 to 0.9) for this flow. Especially there is not any recent investigation in this regard. The aim of his paper is to fulfill this shortcoming.

Mathematical Treatment

Governing Equations: The calculations are based on two-dimensional time-averaged viscous flow equations of motion (Navier-Stokes equations) for perfect gas in non-dimensional conservation form. Both full Navier-Stokes equations and the thin layer approximations were used and in most cases similar results obtained. A transformation is used to map the physical domain onto the computational domain. The non-dimensional parameters governing the flow field such as Reynolds and Mach numbers were defined based on free stream flow properties and the cylinder diameter.

The final form of the non-dimensional equations of motion in a body fitted rectangular coordinate is as follows:

$$\partial_t Q+\partial_\xi E+\partial_\eta F=\mathrm{Re}^{-1}(\partial_\xi E_v+\partial_\eta F_v)$$

where ρ is the density, u and v are the x and y velocity components, e is the total energy, Q is the independent variable vector, E and F are flux terms due to the convection, E_v and F_v are the viscous fluxes and defined as:

$$Q=J^{-1}\begin{bmatrix}\rho\\ \rho u\\ \rho v\\ e\end{bmatrix},\quad E=J^{-1}\begin{bmatrix}\rho U\\ \rho uU+\xi_x p\\ \rho vV+\eta_y p\\ U(e+p)\end{bmatrix},$$

$$F=J^{-1}\begin{bmatrix}\rho V\\ \rho uV+\eta_x p\\ \rho vV+\eta_y p\\ V(e+p)\end{bmatrix}$$

$$E_v = J^{-1}(\xi_x E_v + \xi_y F_v),$$

$$F_v = J^{-1}(\eta_x E_v + \eta_y F_v)$$

U and V are covariant velocities,

$$U_v = (\xi_x u + \xi_y v), V = (\eta_x u + \eta_y v)$$

and J is the Jacobean metric

$$J^{-1} = x_\xi y_\eta - x_\eta y_\xi$$

The pressure is related to the conservative flow variables, Q, by the equation of state

$$p = (\gamma - 1)\left(e - \tfrac{1}{2}\rho(u^2 + v^2)\right)$$

where, γ is the ratio of specific heats. The speed of sound is *a*, which is used to define Mach number and for the ideal gas is, $a^2 = \gamma P/\rho$. The independent parameters ρ, u, v, and e were nondimensionalized based on the free stream quantities ρ_∞ and a_∞.

The Baldwin-Lomax model (1978), which is a conventional two-layer algebraic model, is used to approximate the effects of turbulence. The inner layer is governed by the Prandtl mixing length with Van Driest damping function for the near-wall corrections and the outer layer uses the Closure approximation. The reference mixing length required for the outer layer is calculated from the computed vorticity. No attempt was made to model the wake region, the separated flows and the shock waves.

Numerical Method: Due to the nature of the problem, and the flow structures in the wake region, we employed a time accurate scheme. The initial condition was uniform and the equations were integrated forward in time with time steps commensurate with unsteady phenomena.

The algorithm is an implicit approximate factorization finite difference scheme, which is second order in time. Local linearization was applied to the nonlinear terms and approximate factorization of the two-dimensional implicit operator was used to produce locally one-dimensional operator. The results are block three-diagonal matrices, which are easily solved. The special derivative terms were approximated with second order central differences. An implicit second order and explicit fourth order artificial dissipation terms were used to achieve non-linear stability.

Grid Generations: Two kinds of grid, C- and O-type were generated and used. O-mesh was generated algebraically and the circular grid lines were clustered near the body (Fig. 1). C-mesh was generated using corresponding inviscid flow streamlines and potential lines. These lines are obtained analytically for inviscid flow around a cylinder (Fig. 2). To generate the C-mesh, the flow field is divided into two parts. The O-mesh was used for the first part that contains the inflow plus the first half of the cylinder. For the second part that contains the wake and the other half of the cylinder, a mesh, which coincides with stream function and potential function contours of an inviscid flow around the cylinder was used. The grid was clustered in both directions to resolve shock waves and the large velocity gradient near the cylinder wall.

Results and Discussion

Flows around a cylinder for Reynolds numbers ranged from 10^3 to 8.4 X 10^6 and free stream Mach numbers from 0.1 to 0.9 were studied. In this section, first the grid generation and the validity of the results were discussed. Then the flow configurations around a cylinder were considered. Finally the effects of Reynolds and Mach numbers on the overall flow parameters such as drag and maximum lift coefficients were obtained and discussed.

Computational Grid: Two different grids were used. The grid size in both cases were 121 X 80, but in one case the C-type and in the other case the O-type grid were used. The grids are shown in Fig's 1 and 2 respectively. For Re=1000 and M=0.1, both grids were used to simulate the flow. In both cases the residual dropped to values below 10^{-6} after about 3500 time steps. And the average drag coefficient was identical to three precessions and was 1.260. But as the Mach number were increased, the O-type grid did not give physical results and eventually at Mach numbers greater than about 0.4, the calculation did not converge. So for M>0.4, the C-type mesh was used.

The same flow, Re=1000 and M=0.1, were simulated using different mesh sizes 181 X 120 and 121 X 80. The convergence rate for the bigger mesh was slower as expected. The residual in this case dropped to about 2 X 10^{-6} after about 3000 time steps, whereas the residual for the smaller grid reached 9.0 X 10^{-7}. The average drag coefficients in both cases were 1.260. So 121 X 80 grid were used throughout of the calculations in this paper. The outer diameter in the above-mentioned mesh was 16 cylinder diameters (16D). Fig. 3 shows the centerline velocity behind the cylinder as a function of space for Re=1.4 X 10^4 and M=0.1. As shown in this figure, the centerline velocity curve becomes flat at about 12D. (The cylinder diameter was chosen to be 1 throughout the calculations). So the grid used with 16D was large enough to cover the wake region behind the cylinder.

Simulated Results: The flow around cylinder with three different Reynolds numbers, 10^3, 1.4 X 10^4 and 8.4 X 10^6 and several Mach numbers from 0.1 to 0.9, were simulated. In some cases the results were compared with available data. When no shock waves exist in the flow, that is when the free stream Mach number is less than about 0.5, the residual decreases and becomes about 10^{-7}, after about 3000 to 5000 time steps. But when the shock waves present in the flow, it decreases and reaches the value about 10^{-5}. Fig. 4 shows, as an example, the residual for Re=1000 and M=0.1. The residual decreases to about 10^{-7} after 5000 time steps as shown. In this figure, the residual oscillates and becomes large at time steps between 280 to 600 (the actual non-dimensional time is between 2.8 to 6.0.) The reason is that in this period the cylinder is rotated with linear velocity equal to 1 unit in clockwise direction with the duration of 1.5 unit of time. Then it was stopped for next 0.2 unit of time and again rotated for 1.5 unit of time in

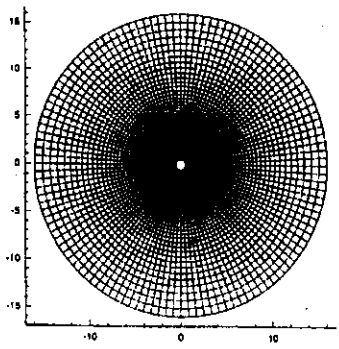

Fig. 1: 121 X 80 O-type grid

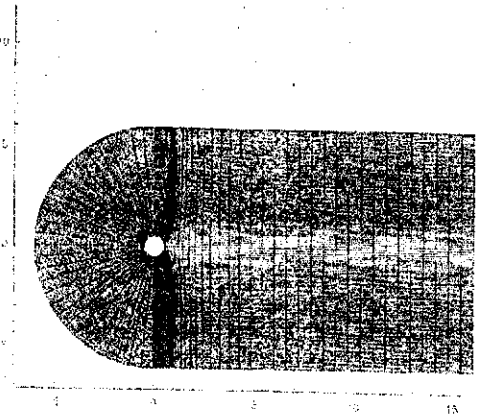

Fig. 2: 121x80 C-type grid

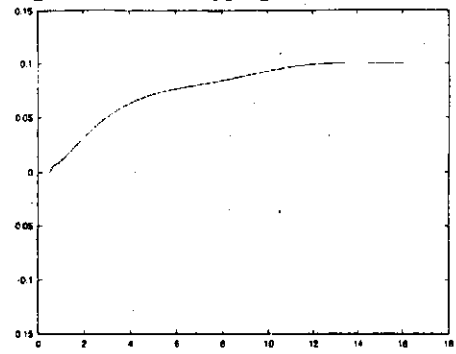

Fig. 3: Center line velocity as a function of distance from center of cylinder

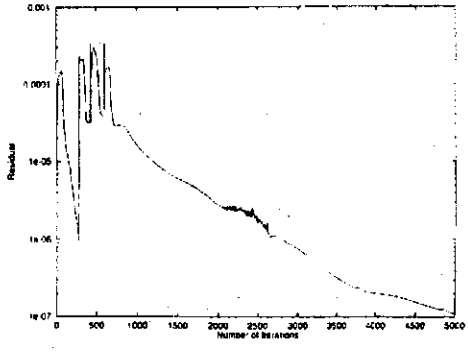

Fig. 4: Residual as a function of number of iterations

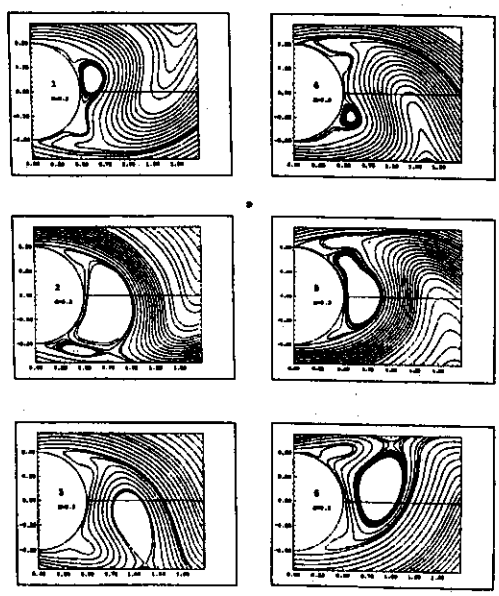

Fig. 5: Stream lines for Re=1000 and M=0.3

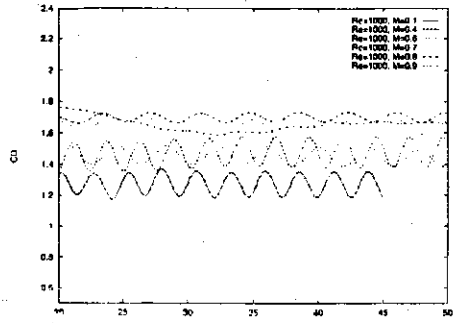

Fig. 6: Drag coefficient for Re=1000

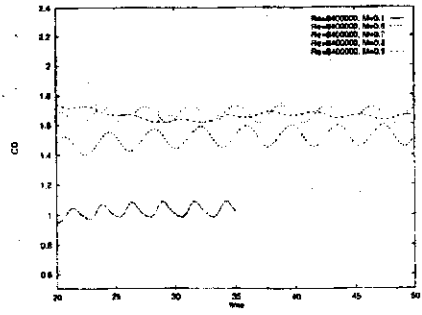

Fig. 7: Drag coefficient for Re=8.4 Ξ 10^6

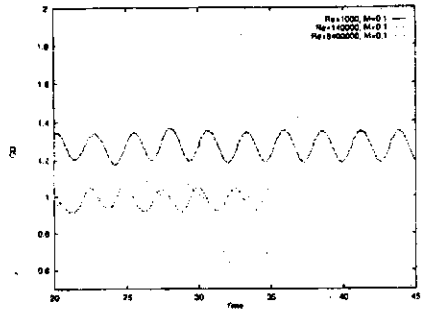

Fig. 8: Drag coefficient for M=0.1

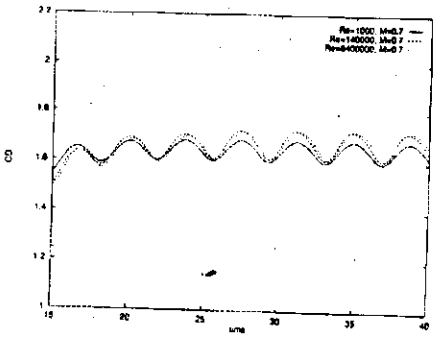

Fig. 9: Drag coefficient for M=0.7

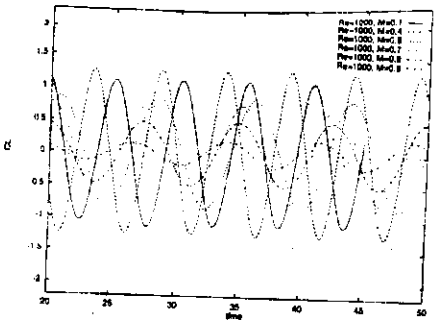

Fig. 10: Lift coefficient for Re=1000

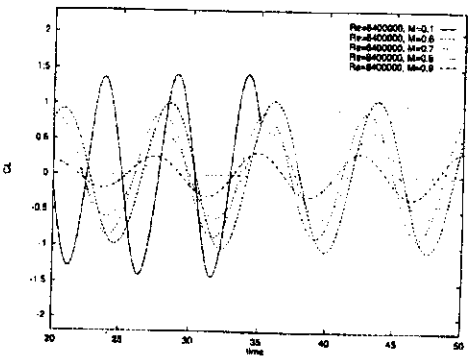

Fig. 11: Lift coefficient for Re=8.4 10^6

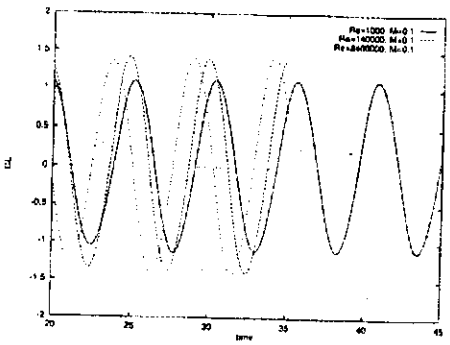

Fig. 12: Lift coefficient for M=0.1

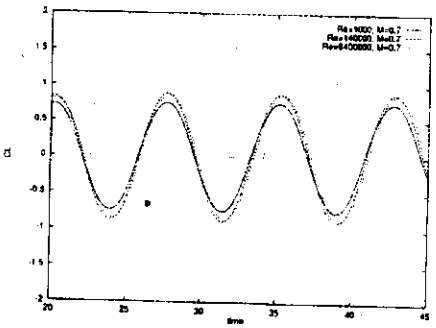

Fig. 13 Lift coefficient for M=0.7

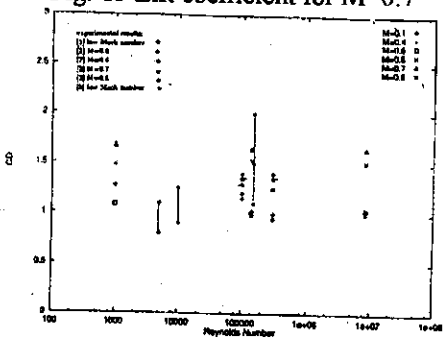

Fig. 14: Average drag Reynolds number

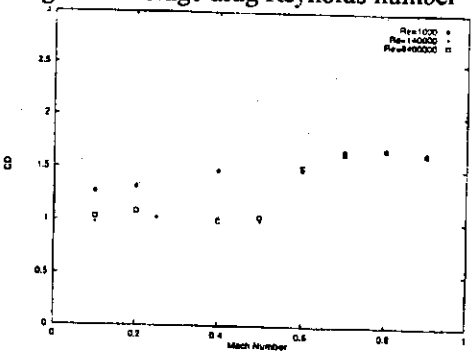

Fig. 15: Average drag as a function of Mach number

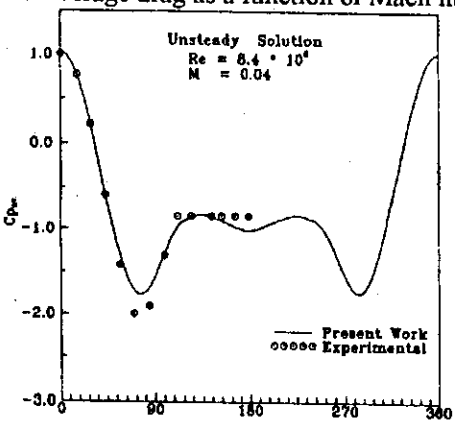

Fig. 16: Average pressure coefficient along the cylinder body

the counter clockwise direction with the same speed. Finally it was stopped for the rest of the calculations. This movement of the cylinder is done, following Braza, *et al.* (1986), in order to obtain unsteady behavior of the flow behind the cylinder in shorter time steps. If this rotation was not done, the unsteady flow, depending on the Mach and Reynolds numbers, would not be obtained within reasonable time steps or it would take much more time steps to develop the unsteady behavior. Fig. 5 shows the streamlines at different times during one period of oscillation for a particular case of Re=1000 and M=0.3. In this figure, the flow structure and the formation and growth of the vortices behind the cylinder is shown. The vortices are generated alternatively from top and bottom part of the flow behind the cylinder. This unsteady behavior causes the oscillations on the various flow characteristics including the instantaneous drag and lift coefficients. Fig's 6 and 7 show the instantaneous drag coefficients as a function of time for Re=1000 and 8.4 X 10^6 respectively. Both the magnitude and frequency of the drag coefficient oscillations vary with Mach number. As Mach number increases, the drag coefficient increases too. But the magnitude and frequency of the oscillations decrease. The increase in drag coefficient is due to the formation of shock waves. As inflow Mach number increases, M>0.5, the local Mach number in some points in the flow field becomes greater than one and the shock waves will be present. Due to the adverse pressure gradient across the shock, the separation point on the cylinder body moves toward the upstream direction, and bigger wake will appear behind the cylinder. This behavior in turns produces larger pressure drag. As the inflow Mach number increases, the sudden decrease in drag coefficient, which is normally seen in incompressible case and is due to the transition of laminar boundary layer to turbulent boundary layer, does not occur. Therefore the displacement of separation point toward the some location down stream does not occur and we do not see this behavior in higher Mach numbers. The main reason is that the shock waves dictate the location of separation points. This phenomenon is clearly shown in the following Figures.

Fig's. 8 and 9 show the drag coefficient as a function of time for Mach numbers of 0.1 and 0.7 respectively. The behavior of variation of drag coefficient at high Mach numbers is very similar even for very different Reynolds numbers. Again this is due to the fact that at high Mach numbers, the dominant parameter is not Reynolds number. Fig's. 10 to 13, show similar results for instantaneous lift coefficient. As shown in the Fig's. 10 and 11, when Mach number increases, both the magnitude and frequency of lift coefficient decreases.

Fig. 14 shows the average drag coefficient as a function of Reynolds number for different Mach numbers. In this figure, the experimental results obtained by others are also shown. The results are well within the experimental results and this shows the validity of the calculations. Fig. 15 shows the drag coefficient as a function of Mach number for different Reynolds numbers. As shown, at about 0.5<M<0.6, the drag coefficient increases by about factors of 1.2 to 1.5, depending on the Reynolds number. But at high Mach numbers, the drag coefficient does not depend on Reynolds number. The drag coefficient increases when the Mach number is in the range of 0. 5 <M <0.8, and then it becomes almost constant for the Mach numbers between 0.8 to 1.0.

Fig. 16 shows the average pressure coefficient on the cylinder body for Re = 8.4 X 10^6 and M=0.04. The results compared with the experimental work done by Cantwell (1983). As shown good agreement is obtained.

Conclusion

Unsteady compressible viscous flows around a circular cylinder were simulated for different Reynolds and Mach numbers. Due to the formation of the wakes behind the cylinder, C-grid is more suitable for this flow. The unsteady behavior of vortices generated causes the oscillations on the various flow characteristics including the instantaneous drag and lift coefficients. The frequency of the oscillations of the drag and lift coefficients depends on the inflow Mach and Reynolds numbers. For M<0.6, the frequency is more effected by Mach number than Reynolds number. In this range the frequency is increased when Mach or Reynolds number decreased. On the other hand for M>0.6, the frequency is not function of Mach number and it is almost constant. When 0.5<M<0.6, the drag coefficient increases very rapidly. It is due to the fact that in this range of inflow Mach number, flow becomes supersonic locally and shock waves appear in the flow. For M>0.6, the drag coefficient does not depend on Reynolds number. It is because in this case, the location of the separation point is dictated by the local shock wave and not by the value of the Reynolds number. Finally, drag coefficient is almost constant when 0.8<M<1.0.

Acknowledgments: This work was done within the framework of the associateship scheme of Abdos Salam International Center for Theoretical Physics (ICTP), Trieste, Italy and is financed by Isfahan University of Technology (IUT). The author would like to thank both IUT and ICTP for their support.

References

Baldwin, B.S. and M. Lomax, 1978. Thin layer approximation and algebraic model for separated turbulent flows, AIAA Paper, No.78-258.

Braza, M., P. Chassaing, and Ha Minh, H. 1986. Numerical study and physical analysis of the pressure and velocity fields in the near wake of a circular cylinder, J. Fluid Mech. 165: 79-103

Cantwell, B., D. Coles, 1983. An experimental study of entrainment and transport in the turbulent near wake of a circular cylinder, J. Fluid Mech., 136: 321-374

Farell, C., J. Blessmann, 1983. On critical flow around smooth circular cylinder, J. Fluid Mech., 136: 375-391

Ferri 1942. Influenza del numero di Reynolds ai grandi numeridi Mach. Atti Guidonia, 67: 68, 69

Schulle-Werning, B., U. Dallmann, B. Muller, 1990. Some aspects of the numerical simulation of compressible flow around bluff bodies at low Mach number, Notes in Numerical Fluid Mechanics 29, Proc. of the eighth GAMM Conf. on Numerical Methods in Fluid Mechanics, 503-512

Song, Charles, C.S., and M. Yuan, 1990. Simulation of vortex shedding flow about a circular cylinder at high Reynolds number, J. Fluid Mech., 112: 155-163.